



Extracellular Synthesis of Metal Nanoparticles by *Claviceps paspali*: Promising Antimicrobial, Anti-Inflammatory, Antiproliferative and Anti-Angiogenic Agents

H. P. Spoorthy^{1,2}, N. Chandra Mohana¹, B. R. Nuthan¹ and S. Satish^{1*}

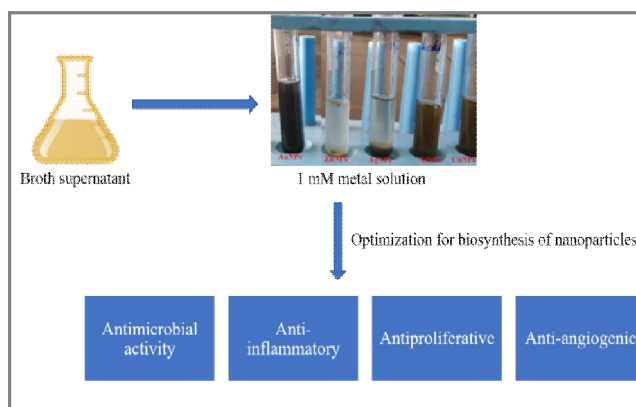
1. DOS in Microbiology, University of Mysore, Mysuru-06, Karnataka, **INDIA**
2. Department of Microbiology, JSS College, B. N. Road, Mysuru-25, Karnataka, **INDIA**
Email: satish.micro@gmail.com

Accepted on 4th April, 2019

ABSTRACT

Extracellular copper, gold, nickel, silver and zinc nanoparticles were biosynthesis from *Claviceps paspali*. The characterization of metal nanoparticles was carried out by using UV-Visible, FT-IR, XRD and SEM spectral analysis. These biosynthesized nanoparticles were showed antimicrobial activity. Few nanoparticles showed significant anti-inflammatory activity. All the nanoparticles exhibited effective antiproliferative and anti-angiogenic activity.

Graphical Abstract



Biosynthesis of nanoparticles and their biological activity.

Keywords: *Claviceps paspali*, Antimicrobial activity, Anti-inflammatory, Antiproliferative, Anti-angiogenic.

INTRODUCTION

Biosynthesis strategies are environmental friendly technique and used in pharmaceutical and different biomedical requisition, as the toxic chemicals are not utilized in those techniques. Synthesis of diverse

nanoparticles by using microbes is used greater than the alternative techniques. Using of environmentally valuable substances such as bacteria, actinomycetes, fungi, yeast, leaf extract of plants and enzymes have been used in nanoparticles synthesis which as a propound benefits of compatibility for pharmaceutic and in different biomedical applications [1]. Copper nanoparticles are gaining interest in medical field of its simplicity when compared to different compounds [2]. At present, gold nanoparticles have attracted tremendous interest inside the field of biology and scientific factors in past few decades [3-6]. Biosynthesized nanoparticles of nickel are extensive biomedical applications [7]. Silver is one of the seven metals of antiquity acknowledged from pre-historic people. It is also found in nature as mixed form with different metals. Zinc nanoparticles are morphologically spherical and an inexperienced crystal [8].

Claviceps paspali also known as ergot fungi because it produces alkaloids that causes ergotism in humans and other mammals when infected grains are consumed [9]. Large-scale production of the ergot alkaloids in submerged culture has been confined solely to the commercially important lysergic acid types produced by *Claviceps paspali* [10]. The present study has shown that the use of *Claviceps paspali* for synthesis of nanoparticles and characterized by different techniques. Furthermore, biological activity was also studied.

MATERIALS AND METHODS

Chemicals required for the biosynthesis of nanoparticles were obtained from SDFCL (Mumbai, India). The bacterial strain used for the nanoparticle synthesis, *Claviceps paspali* (NCIM: 1013) was obtained from NCL, Pune. Culture media and standard antibiotics; muller hinton agar (MHA) potato dextrose broth (PDB), saubaudrod's agar, gentamicin and nystatin, were purchased from Hi Media (Mumbai, India). Human pathogenic cultures of Gram-positive bacteria and Gram-negative bacteria were procured from Microbial Type Culture Collection (MTCC), Chandigarh, India. Pathogenic fungi were procured from DANIDA laboratory, University of Mysore, Mysuru. Cell lines were procured from the National Center for Cell Sciences in Pune, India. All cells were grown in RPMI-1640 supplemented with 10% heat-inactivated FBS, 100 IU mL⁻¹ penicillin, 100 mg mL⁻¹ streptomycin and 2 mM glutamine.

Biosynthesis of nanoparticles: *Claviceps paspali* culture was prepared in potato dextrose broth and saubaudrod's agar maintained at 27°C for 5-7 days. The biomass was harvested and supernatant was collected for further reaction. Supernatant was further treated with 1 mM metal salts such as copper sulphate, gold chloride, nickel chloride, silver nitrate and zinc nitrate and another reaction mixture without metal salts was used as control. The prepared solutions were incubated at 27°C for 24 h. All solutions were kept in dark to avoid any photochemical reactions during the experiment. After, 24 h of incubation observe the colour change. The biosynthesized nanoparticles were purified by centrifugation at 10,000 rpm for 5 min twice and collected for further characterization.

Optimization of nanoparticle biosynthesis

Media: Influence of the culture media on *Claviceps paspali* for the biosynthesis of nanoparticles was determined using potato dextrose agar, cazpek dox's agar and saubaudrod's agar. The yield of the biosynthesized nanoparticles was expressed as µg mL⁻¹.

pH: Nanoparticles biosynthesis was carried out by varying the pH of the reaction mixture at pH 3, 7 and 11 respectively. Optimum pH for the biosynthesis of metal nanoparticles was determined by the yield which was expressed as µg mL⁻¹.

Temperature: The reaction mixture of the metal salts and the cell-free supernatant of *Claviceps paspali* was incubated at three different temperatures at 30°C, 40°C and 50°C respectively. A suitable temperature for the biosynthesis of nanoparticles was determined by monitoring the yield.

Characterization of nanoparticles

UV-Visible spectral analysis: Biosynthesized nanoparticles were studied using Agilent, CARY 60 UV-Vis spectrophotometer absorption spectra through a quartz cuvette with 1 cm path length. Then the surface plasmon resonance characterized against a reference sample [11].

Fourier Transform Infra Red (FT-IR) Spectroscopy: FT-IR analysis determines the functional groups present in biosynthesized nanoparticles. Powdered sample was placed on a 1 mm diameter hole of 0.05 mm thick anti-corrosive steel gasket mounted on a diamond anvil cell of Agilent FT-IR ATR Cary 630. Spectral data was recorded from the range of 7000–350 cm^{-1} with a resolution of 4 cm^{-1} [11].

Scanning Electron Microscopy (SEM) Analysis: Biosynthesized nanoparticles were washed and diluted in distilled water to reach an absorbance range of 0.40 OD. Image analysis was carried out using a drop of bio-nanoparticles layered on a carbon-coated copper and air dried *in-vacuo*. After drying, the bio-nanoparticles were visualized using HITACHI (S-3400N, Japan) with voltage acceleration of 10 kV [11].

X-ray diffraction (XRD) Analysis: XRD measurements of biosynthesized nanoparticles were performed on a Rigaku Desktop Miniflex II X-ray powder diffractometer with Cu α radiation, ($\lambda=1.5406 \text{ \AA}$) as the energy source. The obtained peak positions were compared with standard files to identify the crystalline phase [11]. The size of the particles was calculated using Scherrer's formula:

$$D = \frac{k \lambda}{\beta \cos \theta}$$

Where D is the crystalline size, λ is the wavelength of X-ray used; K is the shape factor, β is the full line width at the half maximum (FWHM) elevation of the main intensity peak, and θ is the Bragg angle. Philips PAN analytical machine was employed for nanoparticles identification using X-ray diffraction studies with a scanning range of 20°-130° and bond angle of 3°.

Antibacterial assay: Antibacterial activity of the biosynthesized nanoparticles was evaluated against seven Gram-negative bacteria (*E. coli*, *K. pneumonia*, *P. mirabilis*, *P. Aerogenosa*, *S. typhimurium*, *S. Paratyphi* and *S. flexneri*) and four Gram-positive bacteria (*B. cereus*, *S. Aureus*, *S. orilies* and *S. mitis*) by disc diffusion assay. Sterile discs (6 mm) were amended with 20 μL of two different concentrations (50 and 100 $\mu\text{g disc}^{-1}$) of nanoparticle solution and placed on the MHA plates, which were previously seeded with standardized test inoculum. Heavy metal solution and CFS used as assay controls (20 $\mu\text{L disc}^{-1}$), gentamicin (10 $\mu\text{g disc}^{-1}$) as positive control respectively [12].

Antifungal activity: Antifungal activity of biosynthesized nanoparticles was evaluated by percent inhibition of pathogenic fungi using poisoned food technique [13]. Biosynthesized nanoparticles were tested against three plant pathogenic fungi *A. niger*, *F. oxysporum* and *H. solani*. Pathogenic fungi were inoculated on to PDA plates previously amended with 50, 100, and 200 $\mu\text{g mL}^{-1}$ concentrations of nanoparticles. The Petri plates containing media devoid of nanoparticle served as assay control, and Nystatin was used as positive control. Petri plates were incubated at $25 \pm 2 \text{ }^\circ\text{C}$ for 7 days, and the colony diameter was measured in mm (Singh and Tirupathi, 1999). Toxicity of the nanoparticles was measured in terms of percentage inhibition of mycelial growth was calculated using the formula,

$$\% \text{ Inhibition} = \frac{C-T}{C} \times 100$$

C= Average increase in mycelia growth in control plate.

T = Average increase in mycelia growth in treatment plate.

Anti-inflammatory assay: A semi-quantitative indirect hemolytic assay was employed to detect the anti-inflammatory activity of the biosynthesized nanoparticles. Briefly, packed human erythrocytes, egg yolk, and phosphate buffer saline was mixed (1:1:8 V/V), and 1ml of this suspension was incubated with 60 μg enzyme for 10 min at 37°C. The reaction was stopped by adding 9 mL of cold phosphate buffer saline and centrifuged at 4°C for 10 min at 800xg. The amount of hemoglobin released in the supernatant was measured at 540 nm [14]. The assay was also carried out in the presence of concentrations of 200 $\mu\text{g mL}^{-1}$ of nanoparticles. Lysis of erythrocytes by adding 9 mL of distilled water to the control reaction mixture was taken as 100%. The resulting turbidity was measured at 600 nm, and the percentage inhibition was calculated as follows, Percentage of inhibition (%) = (OD of Control – OD of Sample/OD of Control) x 100. Diclofenac sodium was used as standard and treated similarly for determination of absorbance.

Antiproliferative activity: The 3-(4,5-dimethylthiazol-2-yl)-2,5-diphenyltetrazolium bromide (MTT) assay was used for the investigation of potential effects of biosynthesized nanoparticles on cell viability [15]. A known number of cells (human cancer cell lines, 5.0×10^3) are transferred into 96 well plates in a volume of 200 μL of culture medium and incubated for 48 hours before the addition of nanoparticles. Cells are then exposed to known concentrations of the biosynthesized nanoparticles to be tested (10 μM expressed as a final concentration) for 24 h at 37°C. After exposure to biosynthesized nanoparticles, the culture medium was removed and 20 μL (diluted in culture medium, 5 mg mL^{-1}) MTT reagent was added. After 4 hours of incubation, MTT reagent was removed, and solvent (100 μL) was added to each well, and plates are agitated for 1 min, and absorbance was recorded at 570 nm. Results are expressed by comparing the absorbance of the wells containing nanoparticle treated cells with the absorbance of wells containing 0.1 % solvent alone.

Anti-angiogenic activity: Chorioallantoic membrane assay was performed according to the method [16]. The fertilized eggs were divided into different treatment groups, which included control, the vehicle-treated group and metal nanoparticle treated groups with a minimum of six eggs in each group. The fertilized eggs were incubated for 6 days at 37°C in a humidified and sterile atmosphere. The window was made on the egg shell to assess the developmental stage of the embryo and was resealed, and incubation was continued. On day 8 the windows were opened, and the compound/vehicle was loaded on the Whatman filter paper discs separately, air dried and inverted over the CAM and the windows were closed. The window was resealed, and the embryo was allowed to develop further. The windows were opened and observed on day 9 and inspected for changes in the micro vessel density in the area around the paper discs.

RESULTS AND DISCUSSION

Optimization of nanoparticle biosynthesis

The effect of media on the production of nanoparticles: The yield of AgNPs was found to be the highest in PDB broth for nanoparticles mediated by *Claviceps paspali* (Table 1). For formation of AuNPs PDB medium was most suitable for fungi there was high yield observed when compared with Cu, Ni and Zn nanoparticles. So, overall from the observed inference, it was inferred PDB for fungi was most suitable for NPs synthesis from the above-mentioned microorganism.

Table 1. Yield of metal nanoparticles ($\mu\text{g mL}^{-1}$) in different media

Test Sample	<i>Claviceps paspali</i>		
	PDB	SDB	CDB
	Yield in $\mu\text{g mL}^{-1}$		
Copper	53.5	51.4	48.5
Gold	58.5	47.0	44.0
Nickel	48.5	47.3	43.2
Silver	59.5	53.5	51.4
Zinc	52.0	48.3	44.2

The effect of pH on the production of nanoparticles: The pH ranges of 3-11 were analyzed for effect of pH and yield. The maximum production was achieved at pH 7 in PDB media for all the metal NPs (Table 2). The yield of Cu NPs was found to be the highest in pH 7 for *Claviceps paspali*. The effect of pH did not influence copper NPs synthesis; the change in yield was insignificant. For formation of Gold NPs, Nickel NPs, Silver NPs and Zinc NPs exhibited a slight increase in yield for pH variations. The overall results indicated that even though a slight increase in the yield for pH 7 observed for the microorganism in the study, it can be concluded that the pH 7 to be most favorable for NP synthesis.

Table 2. The effect of pH on the production of nanoparticles

Test Sample	<i>Claviceps paspali</i>		
	pH 3	pH 7	pH 11
	Yield in $\mu\text{g mL}^{-1}$		
Copper	50.1	51.4	48.5
Gold	57.7	61.5	54.4
Nickel	46.0	49.3	43.2
Silver	59.4	63.5	56.4
Zinc	46.0	48.8	44.0

Effect of temperature on the growth of the microorganism: The varying temperature of 30°C, 40°C and 50°C was employed to determine the maximum yield. Microorganism produces maximum amount of silver nanoparticles at 40 °C in PDB media (Table 3). This result indicated that elevated temperature influenced the synthesis of nanoparticles.

Table 3. Effect of temperature nanoparticles

Test Sample	<i>Claviceps paspali</i>		
	30°C	40°C	50°C
	Yield in $\mu\text{g mL}^{-1}$		
Copper	40.5	51.0	48.7
Gold	55.3	61.5	58.0
Nickel	43.0	49.7	45.2
Silver	56.4	64.3	58.8
Zinc	57.0	61.3	60.3

on the production of

UV-Visible spectral analysis: Metal nanoparticles were ascertaining with supernatant of fungal culture *Claviceps paspali* which reduced metal salts to metal nanoparticles as shown in figure 1 with maximum absorption between 370 to 575 nm with a broad and prominent peak and the synthesis was

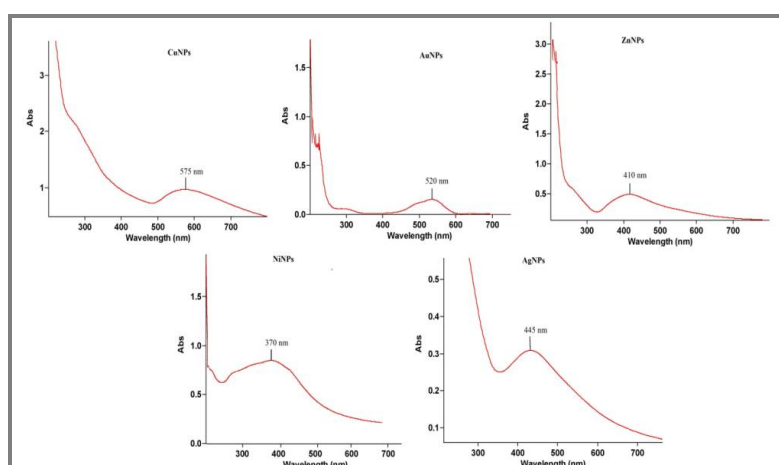


Figure 1. UV-Visible spectrum of metal nanoparticles mediated by *Claviceps paspali*.

achieved within 24 h of incubation time. An absorption peak was observed at 575 nm and is an indication of formation of CuNPs. AuNPs showed maximum absorption at 520 nm, NiNPs at 370 nm, AgNPs at 445 nm and ZnNPs showed maximum peak absorption at 410 nm.

Fourier Transform Infra-Red (FT-IR) Spectroscopy: FT-IR analysis of metal nanoparticles synthesized by *Claviceps paspali* culture resulted in predominant peaks, the N-H stretching observed at $3279\text{-}2919\text{ cm}^{-1}$, which confirms the amide group (Figure 2). The spectral region at $1626\text{ to }1622\text{ cm}^{-1}$ is C=O stretching and $1539\text{-}1327\text{ cm}^{-1}$ C-N stretching of above six nanoparticles. The spectral region at $1200\text{-}900\text{ cm}^{-1}$ contains absorption bands of the carbonyl group in microbial cell walls. The C-O band was observed at $1055\text{ to }1015\text{ cm}^{-1}$ and C=O bending frequency is $550\text{ to }477\text{ cm}^{-1}$. The presence of amines, carbonyl and amide, are known to facilitate the synthesis and stabilization of nanoparticles.

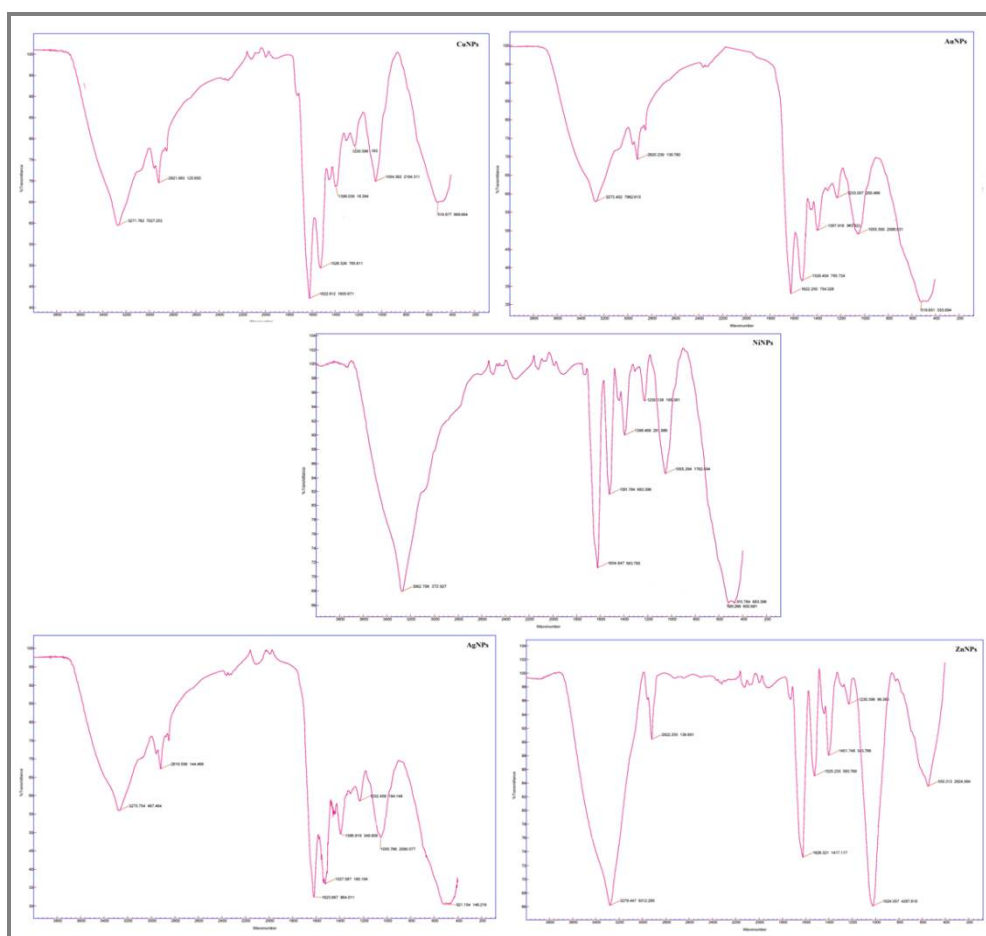


Figure 2. FT-IR analysis of metal nanoparticles mediated by *Claviceps paspali*.

Scanning Electron Microscopy (SEM) Analysis: In *Claviceps paspali*, CuNPs showed at $30\text{ }\mu\text{m}$ with magnification of 5.00 KX, AuNPs showed magnification of 1.00 KX with particle size at $10\text{ }\mu\text{m}$, NiNPs showed the particle size at $1\text{ }\mu\text{m}$ with magnification of 10.00 KX, particle size of the AgNPs at $1\text{ }\mu\text{m}$ with magnification of 4.00 KX and ZnNPs is $30\text{ }\mu\text{m}$ with magnification of 500 X.

X-ray diffraction (XRD) Analysis: The XRD pattern exhibited the crystalline nature of metal nanoparticles using supernatant *Claviceps paspali* culture. The diffraction intensities occurring at 2θ values which correspond to (111), (200), (220) and (311) of lattice plane of face-centered cubic (fcc) of nanoparticles. The XRD pattern clearly showed that the synthesized metal nanoparticles formed were composed of pure crystalline and formed by the reduction of metal ions.

Antibacterial assay: The antibacterial of biosynthesized metal NPs revealed the biosynthesized metal NPs were effective against all test pathogens (Table 4). Cu NPs showed maximum inhibition against *Streptococcus oralis* and *Pseudomonas aeruginosa* inhibition was least for *Streptococcus mitis*. Au NPs had a maximum inhibitory effect against *Staphylococcus aureus* followed by *Streptococcus mitis* was least effective against *Bacillus cereus* and *Salmonella paratyphi*. The Ni NPs inhibited *Escherichia coli* significantly followed by *Pseudomonas aeruginosa*, *Salmonella paratyphi*. The Ag NPs were found to be most effective against *Pseudomonas aeruginosa*, but was found to be less significant against *Escherichia coli*. Zn NPs were found to be most effective against *Pseudomonas aeruginosa* followed by *Staphylococcus aureus* and *Escherichia coli* were found to be least against *Streptococcus mitis*.

Table 4. *In vitro* antibacterial activity of metal nanoparticles against *Claviceps paspali*

Test sample	Conc. $\mu\text{g disc}^{-1}$	Zone of Inhibition in mm										
		<i>B. cereus</i>	<i>S. aureus</i>	<i>S. mitis</i>	<i>S. oralis</i>	<i>E. coli</i>	<i>K. pneumonia</i>	<i>P. mirabilis</i>	<i>P. aeruginosa</i>	<i>S. paratyphi</i>	<i>S. typhimurium</i>	<i>S. flexneri</i>
Copper	Control	10.00 \pm 1.00 ^{hi}	10.00 \pm 1.00 ^{jk}	10.33 \pm 0.58 ^{hij}	8.67 \pm 0.58 ^{hi}	8.33 \pm 0.58 ^h	9.33 \pm 0.58 ^g	9.00 \pm 1.00 ^{fg}	11.00 \pm 1.00 ^{hi}	9.00 \pm 1.00 ⁱ	9.00 \pm 1.00 ^{hi}	8.00 \pm 1.00 ^h
	50	15.33 \pm 0.58 ^{de}	20.00 \pm 1.00 ^{cd}	11.67 \pm 0.58 ^{ghi}	22.00 \pm 1.00 ^b	15.67 \pm 0.58 ^{bcd}	19.67 \pm 0.58 ^{cd}	11.67 \pm 0.58 ^{de}	21.33 \pm 0.58 ^c	19.33 \pm 0.58 ^{bc}	13.67 \pm 0.58 ^{de}	11.33 \pm 0.58 ^{fg}
	100	18.00 \pm 1.00 ^c	22.67 \pm 0.58 ^{ab}	14.00 \pm 1.00 ^{fg}	24.67 \pm 0.58 ^a	18.00 \pm 1.00 ^b	22.33 \pm 0.58 ^{ab}	13.67 \pm 0.58 ^{cd}	24.33 \pm 0.58 ^a	21.67 \pm 0.58 ^{ab}	16.67 \pm 0.58 ^c	17.00 \pm 1.00 ^{bc}
Gold	Control	9.00 \pm 1.00 ^{ij}	9.00 \pm 1.00 ^k	8.00 \pm 1.00 ^j	9.33 \pm 0.58 ^{ghi}	8.00 \pm 1.00 ^h	9.00 \pm 1.00 ^g	8.67 \pm 0.58 ^{fg}	10.00 \pm 1.00 ⁱ	9.67 \pm 0.58 ^{hi}	7.67 \pm 0.58 ⁱ	8.00 \pm 1.00 ^h
	50	11.67 \pm 0.58 ^{fgh}	22.33 \pm 0.58 ^{ab}	19.33 \pm 0.58 ^{bc}	12.67 \pm 0.58 ^{ef}	14.67 \pm 0.58 ^{cde}	15.00 \pm 1.00 ^{ef}	13.00 \pm 1.00 ^{cd}	14.33 \pm 0.58 ^{fg}	14.67 \pm 0.58 ^f	11.67 \pm 0.58 ^{efg}	12.33 \pm 0.58 ^{ef}
	100	14.00 \pm 1.00 ^{ef}	24.33 \pm 0.58 ^a	22.67 \pm 0.58 ^a	17.00 \pm 1.00 ^d	16.33 \pm 0.58 ^{bc}	17.67 \pm 0.58 ^{cd}	17.00 \pm 1.00 ^b	16.67 \pm 0.58 ^{de}	18.00 \pm 1.00 ^{cd}	14.00 \pm 1.00 ^{de}	15.33 \pm 0.58 ^{cd}
Nickel	Control	10.67 \pm 0.58 ^{ghi}	8.33 \pm 0.58 ^k	10.00 \pm 1.00 ^{ij}	9.67 \pm 0.58 ^{ghi}	9.00 \pm 1.00 ^h	8.67 \pm 0.58 ^g	8.33 \pm 0.58 ^g	12.67 \pm 0.58 ^{gh}	11.00 \pm 1.00 ^{hi}	10.67 \pm 0.58 ^{fgh}	9.00 \pm 1.00 ^{gh}
	50	14.00 \pm 1.00 ^{ef}	18.33 \pm 0.58 ^{de}	16.33 \pm 0.58 ^{def}	17.67 \pm 0.58 ^{cd}	16.00 \pm 1.00 ^{bcd}	13.67 \pm 0.58 ^f	14.00 \pm 1.00 ^e	18.00 \pm 1.00 ^d	15.67 \pm 0.58 ^{def}	14.00 \pm 1.00 ^{de}	14.00 \pm 1.00 ^{de}
	100	19.00 \pm 1.00 ^{bc}	20.67 \pm 0.58 ^{bc}	20.67 \pm 0.58 ^{ab}	21.67 \pm 0.58 ^b	23.00 \pm 1.00 ^a	20.00 \pm 1.00 ^{bc}	18.33 \pm 0.58 ^{ab}	22.33 \pm 0.58 ^{abc}	22.00 \pm 1.00 ^a	21.33 \pm 0.58 ^{ab}	19.00 \pm 1.00 ^{ab}
Silver	Control	13.00 \pm 1.00 ^{efg}	10.67 \pm 0.58 ^{ij}	12.00 \pm 1.00 ^{ghi}	11.00 \pm 1.00 ^{fg}	15.67 \pm 0.58 ^{bcd}	12.67 \pm 0.58 ^f	10.67 \pm 0.58 ^{ef}	15.33 \pm 0.58 ^{ef}	8.67 \pm 0.58 ⁱ	10.67 \pm 0.58 ^{fgh}	8.33 \pm 0.58 ^h
	50	17.67 \pm 0.58 ^{cd}	12.67 \pm 0.58 ^{hi}	15.33 \pm 0.58 ^{ef}	19.33 \pm 0.58 ^c	12.00 \pm 1.00 ^{fg}	22.67 \pm 0.58 ^a	13.33 \pm 0.58 ^{cd}	18.67 \pm 0.58 ^d	11.67 \pm 0.58 ^{gh}	9.00 \pm 1.00 ^{hi}	10.00 \pm 1.00 ^{fgh}
	100	22.00 \pm 1.00 ^a	16.00 \pm 1.00 ^{fg}	18.00 \pm 1.00 ^{cd}	21.67 \pm 0.58 ^b	13.67 \pm 0.58 ^{def}	23.33 \pm 0.58 ^a	17.00 \pm 1.00 ^b	23.33 \pm 0.58 ^{abc}	14.00 \pm 1.00 ^{fg}	12.67 \pm 0.58 ^{def}	15.00 \pm 1.00 ^{cd}
Zinc	Control	11.00 \pm 1.00 ^{ghi}	15.00 \pm 1.00 ^g	9.00 \pm 1.00 ^j	10.33 \pm 0.58 ^{gh}	11.67 \pm 0.58 ^{fg}	9.00 \pm 1.00 ^g	8.67 \pm 0.58 ^{fg}	13.67 \pm 0.58 ^{fg}	11.00 \pm 1.00 ^{hi}	9.00 \pm 1.00 ^{hi}	9.00 \pm 1.00 ^{gh}
	50	15.33 \pm 0.58 ^{de}	19.33 \pm 0.58 ^{cde}	11.67 \pm 0.58 ^{ghi}	13.00 \pm 1.00 ^{ef}	14.67 \pm 0.58 ^{cde}	15.00 \pm 1.00 ^{ef}	14.33 \pm 0.58 ^c	18.67 \pm 0.58 ^d	15.33 \pm 0.58 ^{ef}	20.00 \pm 1.00 ^{ab}	11.67 \pm 0.58 ^{ef}
	100	18.00 \pm 1.00 ^c	22.33 \pm 0.58 ^{ab}	14.00 \pm 1.00 ^g	16.67 \pm 0.58 ^d	17.00 \pm 1.00 ^{bc}	17.33 \pm 0.58 ^{de}	18.33 \pm 0.58 ^{ab}	23.67 \pm 0.58 ^{ab}	18.00 \pm 1.00 ^{cd}	22.33 \pm 0.58 ^a	14.00 \pm 1.00 ^{de}
Gentamicin	10	21.00 \pm 1.00 ^{ab}	22.67 \pm 0.58 ^{ab}	20.67 \pm 0.58 ^{ab}	22.00 \pm 1.00 ^b	23.00 \pm 1.00 ^a	19.00 \pm 1.00 ^{cd}	20.33 \pm 0.58 ^a	22.00 \pm 1.00 ^{bc}	19.67 \pm 0.58 ^{abc}	20.33 \pm 0.58 ^{ab}	21.00 \pm 1.00 ^a
Culture filtrate	25 μL	0.00 \pm 0.00 ^k	0.00 \pm 0.00 ^l	0.00 \pm 0.00 ^k	0.00 \pm 0.00 ^j	0.00 \pm 0.00 ⁱ	0.00 \pm 0.00 ^h	0.00 \pm 0.00 ^h	0.00 \pm 0.00 ^j	0.00 \pm 0.00 ^j	0.00 \pm 0.00 ^j	0.00 \pm 0.00 ⁱ

Values expressed are means of triplicates \pm standard deviation of the mean (SDM; significant $p < 0.001$) by one-way ANOVA, followed by the same superscript letter(s) within columns are significantly different at $p < 0.05$ by Tukey's post hoc test.

Antifungal activity: There was no antifungal activity observed by Cu NPs, Ni NPs and Zn NPs at a lower concentration, but activity was observed at a concentration of 100 $\mu\text{g mL}^{-1}$ (Table 5). There was no inhibition of *Aspergillus niger* by Ni NPs observed even at higher concentrations. The Cu NPs

were most inhibitory against *Fusarium oxysporum* followed by *Aspergillus niger* and *Helminthosporium solani*. Biosynthesized Zn NPs and Ag NPs had a similar inhibitory effect against all fungal test pathogens.

Table 5. *In vitro* antifungal activity of metal nanoparticles against *Claviceps paspali*

Test Sample	Conc. ($\mu\text{g mL}^{-1}$)	% Inhibition		
		<i>Aspergillus niger</i>	<i>Fusarium oxysporum</i>	<i>Helminthosporium solani</i>
Copper	50	NIL	NIL	NIL
	100	61.66 \pm 0.60 ^g	68.26 \pm 0.69 ^d	63.30 \pm 0.95 ^{fg}
	200	66.15 \pm 0.84 ^f	69.21 \pm 0.62 ^d	62.23 \pm 0.48 ^g
Gold	50	70.23 \pm 0.69 ^e	44.12 \pm 0.69 ^h	72.91 \pm 0.58 ^{de}
	100	72.51 \pm 0.76 ^d	61.39 \pm 0.54 ^f	74.75 \pm 0.57 ^{cd}
	200	74.45 \pm 0.57 ^c	75.13 \pm 0.74 ^b	75.28 \pm 0.54 ^c
Nickel	50	NIL	NIL	NIL
	100	NIL	31.14 \pm 0.90 ⁱ	71.26 \pm 1.01 ^e
	200	NIL	71.32 \pm 1.14 ^c	71.27 \pm 0.86 ^e
Silver	50	70.18 \pm 0.66 ^e	44.47 \pm 0.83 ^h	72.22 \pm 0.95 ^e
	100	74.45 \pm 0.78 ^c	61.26 \pm 0.84 ^f	75.16 \pm 0.84 ^e
	200	74.80 \pm 0.67 ^c	74.81 \pm 0.48 ^b	74.28 \pm 0.48 ^{cd}
Zinc	50	NIL	NIL	NIL
	100	64.93 \pm 0.78 ^f	64.49 \pm 0.64 ^e	64.82 \pm 0.70 ^f
	200	65.32 \pm 0.81 ^f	65.04 \pm 0.56 ^e	64.79 \pm 0.58 ^f
Nystatin	50	82.17 \pm 0.73 ^b	68.45 \pm 0.79 ^d	84.16 \pm 0.59 ^b
	100	85.17 \pm 0.79 ^a	73.42 \pm 0.67 ^b	87.11 \pm 0.73 ^a
	200	85.13 \pm 0.59 ^a	80.13 \pm 0.56 ^a	86.70 \pm 0.65 ^a

Values expressed are means of triplicates \pm standard deviation of the mean (SDM; significant $p < 0.001$) by one-way ANOVA, followed by the same superscript letter(s) within columns are significantly different at $p < 0.05$ by Tukey's post hoc test.

Anti-inflammatory assay: In *Claviceps paspali*, both Au NPs and Zn NPs exhibited good anti-inflammatory activity with IC_{50} value of 35 followed by Cu NPs, Ag NPs and Ni NPs. From the study results, we can conclude that Au NPs and Zn NPs were most suitable candidates for anti-inflammatory activity (Table 6).

Table 6. IC_{50} value of PLA_2 Inhibition by different metal nanoparticles

Test sample	IC_{50} $\mu\text{g mL}^{-1}$
Copper	53.04 \pm 1.50
Gold	35.05 \pm 1.12
Nickel	61.51 \pm 1.15
Silver	56.02 \pm 1.50
Zinc	35.56 \pm 1.13
Diclofenac sodium	12.80 \pm 1.38

Note: Values given are mean of triplicates \pm S. E. M. (significant $p < 0.001$).

Antiproliferative activity: The percentage of cell survival for *Claviceps paspali* mediated Cu NPs were highest against Colo-205 and IMR-32 cell lines followed by MDA-MB 231 and K562 cell line (Table 7). In case of *Claviceps paspali* mediated Au NPs was found to be effective against Colo-205 cell lines with survival percentage of 74% followed by MDA-MB 231, IMR-32 and K562 cell lines with survival percentage of 71%, 67% and 60% respectively. The Ni NPs were most effective in case of Colo-205 followed by MDA-MB 231. The *Claviceps paspali* mediated Ag NPs showed highest survival for both MDA-MB 231 and Colo-205 cell lines followed by IMR-32 and K562 cell line. For *Claviceps paspali* mediated Zn NPs survival was found to be highest against Colo 205 followed by MDA-MB 231, K562 and IMR-32.

Table 7. Antiproliferative activity (in %) of metal NPs determined by MTT test

Test sample	Cell lines	<i>Claviceps paspali</i>
		% cell survival at 10 μ M
Copper	MDA-MB 231	64.12 \pm 0.20
	K562	58.01 \pm 0.21
	Colo-205	66.20 \pm 0.03
	IMR-32	66.21 \pm 0.31
Gold	MDA-MB 231	71.22 \pm 0.10
	K562	60.32 \pm 0.21
	Colo-205	74.31 \pm 0.34
	IMR-32	67.12 \pm 0.05
Nickel	MDA-MB 231	59.20 \pm 0.23
	K562	55.42 \pm 0.11
	Colo-205	61.20 \pm 0.10
	IMR-32	56.16 \pm 0.25
Silver	MDA-MB 231	75.51 \pm 0.11
	K562	62.21 \pm 0.24
	Colo-205	75.10 \pm 0.24
	IMR-32	66.70 \pm 0.32
Zinc	MDA-MB 231	60.42 \pm 0.21
	K562	56.10 \pm 0.23
	Colo-205	61.34 \pm 0.10
	IMR-32	55.32 \pm 0.32
DMSO (Control)	MDA-MB 231	99.90 \pm 0.02
	K562	99.90 \pm 0.02
	Colo-205	99.90 \pm 0.02
	IMR-32	99.90 \pm 0.02

Note: Values given are mean of triplicates \pm S. E. M. (significant $p < 0.001$).

Anti-angiogenic activity: The investigation of anti-angiogenic activity of *Claviceps paspali* mediated nanoparticles in chorioallantoic membrane (CAM) assay showed significant reduction of proliferation of capillaries around the zone of application of the discs loaded with the nanoparticles as compared to the control site where only the vehicle, 0.1% polyethylene glycol (PEG) were applied. These results indicate that the metal nanoparticles are potent anti-angiogenic molecules. The angio-inhibitory activity of the metal nanoparticles is as shown in the exhibiting significant positive results in the CAM assay model of developing embryos.

Thus, the present study shows the significance of metal nanoparticles synthesized from fungi. Interestingly, silver nanoparticles were found to be more potent with regard to antibacterial activity, antifungal activity, anti-inflammatory activity, and antiproliferative activity followed gold nanoparticles. The biogenic synthesis could be concluded as a potential alternate for synthesizing nanoparticles with less toxicity and enhanced biocompatibility.

APPLICATION

The biogenic synthesis could be concluded as a potential alternate for synthesizing nanoparticles with less toxicity and enhanced biocompatibility. Therefore, from this study, we can conclude that bio-fabricated nanomaterials have the potential for therapeutic applications.

CONCLUSION

Metal nanoparticles were successfully synthesized using microorganisms. Antimicrobial property reveals that few nanoparticles showed good activity also exhibited good anti-inflammatory property. These exhibited significant antiproliferation against cell lines and all the NPs showed significant positive results in this model of developing embryos. Therefore, from this study, we can conclude that bio-fabricated nanomaterials have the potential for therapeutic applications.

ACKNOWLEDGEMENTS

The authors are thankful to the DOS in Microbiology, Manasagangotri, University of Mysore and JSS College, Mysuru, India for providing facility and infrastructure.

REFERENCES

- [1]. M. A. Willard, L. K. Kurihara, E. E. Carpenter, S. Calvin, V. G. Harris, Chemically prepared magnetic nanoparticles, *Inter. Mat. Rev.*, **2004**, 49, 125-170.
- [2]. S. Honary, H. Barabadi, E. G. Fathabad, F. Naghibi, Green synthesis of silver nanoparticles induced by the fungus *penicillium citrinum*, *Digest J. Nano. Biostru*, **2012**, 7, 999-1005.
- [3]. H. Barabadi, S. Honary, P. Ebrahimi, M. A. Mohammadi, A. Alizadeh, F. Naghibi, Microbial mediated preparation, characterization and optimization of gold nanoparticles, *Braz J Micro.*, **2014**, 45(4), 1493-1501.
- [4]. P. Mukherjee, Roy M, B. P. Mandal, G. K. Dey, P. K. Mukherjee, J. Ghatak, A. K. Tyagi, S. P. Kale, Green synthesis of highly stabilized nanocrystalline silver particles by a non pathogenic and agriculturally important fungus *T. asperellum*, *Nanotech.*, **2008**, 19(7), 075103-075110.
- [5]. C. R. Patra, R. Bhattacharya, D. Mukhopadhyay, P. Mukherjee, Fabrication of gold nanoparticles for targeted therapy in pancreatic cancer, *Adv. Drug Del. Rev.*, **2010**, 62(3), 346-361.
- [6]. A. Ahmad, S. Senapati, M. I. Khan, Intracellular synthesis of gold nanoparticles by a novel alkalotolerant actinomycete, *Rhodococcus* species, *Nanotech.*, **2003**, 14(7), 824-828.
- [7]. S. A. El-Debaiky, A. S. M. El-Badry, M. M. El-Shahaw, Biosynthesis of nickel oxide nanoparticles using *fusarium verticillioides* (Sacc.) and their biological activity against some causative agents of mycotic keratitis, *Egypt J. Bot.*, **2017**, 57(3), 417-428.
- [8]. K. H. Kumar, V. P. Savalgi, Microbial synthesis of zinc nanoparticles using fungus isolated from rhizosphere soil, *Int. J. Curr. Microbiol. App. Sci.*, **2017**, 6(12), 2359-2364.
- [9]. R. J. Cole, J. W. Dorner, J. A. Lansden, Paspalum staggers: Isolation and identification of tremorgenic metabolites from sclerotia of *Claviceps paspali*, *J. Agric. Food Chem.*, **1977**, 25 (5), 1197-1201.
- [10]. F. Arcamone, E. B. Chain, A. Ferretti, A. Minghetti, P. Pennella, A. Tonolo, L. Vero, Production of a new lysergic acid derivative in submerged culture by a strain of *clavicepspaspali stevens and hall*, *Proceedings of the Royal Society B*, **1961**, 155, 26-54.
- [11]. S. Sandeep., A. S. Santhosh., N. K. Swamy., G. S. Suresh, J. S. Melo., P. Mallu. Biosynthesis of silver nanoparticles using *Convolvulus pluricaulis* leaf extract and assessment of their catalytic, electrocatalytic and phenol remediation properties, *Adv. Mater. Lett.*, **2016**, 7(12), 383-389.
- [12]. J. D. Pascal., K. Stanich, B. Girard, G. Mazza, Antimicrobial activity of individual and mixed fractions of dill, cilantro, coriander and eucalyptus essential oils, *Inter. J. Food Microbio.*, **2002**, 74(1), 101-109.
- [13]. N. Khandelwal, A. Singh, D. Jain, M. K. Upadhyay, H. N. Verma, Green synthesis of silver nanoparticles using *Argemone Mexicana* leaf extract and evaluation of their antimicrobial activities, *Digest Journal of Nanomaterials and Biostructures*, **2010**, 5(2), 483-489.
- [14]. O. H. Lowry, N. J. Rosenbrough, A. L. Farr, R. J. Randall, Protein measurement with the Folin phenol reagent, *J. Biol. Chem.*, **1951**, 193(1), 265-275.
- [15]. T. Mosmann, Rapid colorimetric assay for cellular growth and survival, application to proliferation and cytotoxicity assays, *J. Immunol. Methods*, **1983**, 65(1-2), 55-63.
- [16]. P. Nowak-Sliwinska, T. M. L. Segura, The chicken chorioallantoic membrane model in biology, medicine and bioengineering, *Angiogenesis*, **2014**, 17(4), 779-804.